AMERICAN SOCIETY FOR MICROBIOLOGY | Infection and Immunity®

BACTERIAL INFECTIONS

Studies of *Streptococcus anginosus* Virulence in *Dictyostelium discoideum* and *Galleria mellonella* Models

Joanna Budziaszek,[a] Magdalena Pilarczyk-Zurek,[a] Ewelina Dobosz,[a] Aleksandra Kozinska,[b] Dariusz Nowicki,[a,c] Katarzyna Obszanska,[b] Agnieszka Szalewska-Pałasz,[c] Izabela Kern-Zdanowicz,[d] Izabela Sitkiewicz,[e] Joanna Koziel[a]

[a]Department of Microbiology, Faculty of Biochemistry, Biophysics and Biotechnology, Jagiellonian University, Krakow, Poland
[b]Department of Drug Biotechnology and Bioinformatics, National Medicines Institute, Warsaw, Poland
[c]Department of Molecular Biology, University of Gdańsk, Gdańsk, Poland
[d]Institute of Biochemistry and Biophysics, Polish Academy of Sciences, Warsaw, Poland
[e]Institute of Biology, Warsaw University of Life Sciences-SGGW, Warsaw, Poland

ABSTRACT For many years, *Streptococcus anginosus* has been considered a commensal colonizing the oral cavity, as well as the gastrointestinal and genitourinary tracts. However, recent epidemiological and clinical data designate this bacterium as an emerging opportunistic pathogen. Despite the reported pathogenicity of *S. anginosus*, the molecular mechanism underpinning its virulence is poorly described. Therefore, our goal was to develop and optimize efficient and simple infection models that can be applied to examine the virulence of *S. anginosus* and to study host-pathogen interactions. Using 23 *S. anginosus* isolates collected from different infections, including severe and superficial infections, as well as an attenuated strain devoid of CppA, we demonstrate for the first time that *Dictyostelium discoideum* is a suitable model for initial, fast, and large-scale screening of virulence. Furthermore, we found that another nonvertebrate animal model, *Galleria mellonella*, can be used to study the pathogenesis of *S. anginosus* infection, with an emphasis on the interactions between the pathogen and host innate immunity. Examining the profile of immune defense genes, including antimicrobial peptides, opsonins, regulators of nodulation, and inhibitors of proteases, by quantitative PCR (qPCR) we identified different immune response profiles depending on the *S. anginosus* strain. Using these models, we show that *S. anginosus* is resistant to the bactericidal activity of phagocytes, a phenomenon confirmed using human neutrophils. Notably, since we found that the data from these models corresponded to the clinical severity of infection, we propose their further application to studies of the virulence of *S. anginosus*.

KEYWORDS *Streptococcus anginosus*, *Galleria mellonella*, *Dictyostelium discoideum*, virulence, infection models, neutrophils

Streptococcus anginosus, along with *Streptococcus constellatus* and *Streptococcus intermedius*, belongs to the *Streptococcus anginosus* group. Initially, this group was classified as the primary commensal of the mucosal membranes of the oral cavity, but it can also colonize the throat, nasopharynx, gastrointestinal tract, and genitourinary tract (1). Improved diagnostic methods revealed that this species of *streptococcus* has extensive pathogenic potential; indeed, a growing number of life-threatening infections have been documented in clinical practice. *S. anginosus* is frequently found in cases of bacteremia (2), liver abscess, and gastrointestinal and genitourinary tract infections (3). Although clinical data indicate that *S. anginosus* should be considered an opportunistic pathogen, few studies have examined its virulence strategies (3).

Data from available virulence and comparative genomic-sequencing studies revealed that *S. anginosus* encodes putative virulence factors common to other streptococci; these

Editor Nancy E. Freitag, University of Illinois Chicago

Address correspondence to Joanna Koziel, joanna.koziel@uj.edu.pl, or Magdalena Pilarczyk-Zurek, magdalena.pilarczyk-zurek@uj.edu.pl.

The authors declare no conflict of interest.

Received 15 January 2023
Returned for modification 13 February 2023
Accepted 29 March 2023

include hemolysins (4) adhesins (5), DNases (6), the capsule (7), toxins (8), pili (9), hyaluronidases (10), enolases (9), and superantigens (6). Although their role in the pathogenicity of *S. anginosus* has been postulated, experimental evidence is lacking. The majority of data that describe the role of putative determinants of *S. anginosus* virulence comes from *in vitro* studies (11, 12), while the real mechanisms underlying the bacterial interaction with the host remain unknown, primarily due to a lack of efficient animal models.

Dictyostelium discoideum is a simple, unicellular eukaryotic model system that has been developed to screen for bacterial virulence. The model has been exploited mainly to study the pathogenic potential of Gram-negative species, including *Vibrio cholerae* (13), *Aeromonas hydrophila* (14), *Pseudomonas aeruginosa* (15, 16), *Burkholderia cenocepacia* (17), and *Burkholderia pseudomallei* (18), as well as Gram-positive bacteria, such as *Mycobacterium marinum* (19). Among streptococcal species, only *Streptococcus suis* was examined in the described model (20). More importantly, a *D. discoideum* model provides the ability to track the infection process at the level of genetic and biochemical interactions using well-established tools (21–24). The vast availability of amoeba mutant strains allows the evaluation of pathogen-host interactions at the molecular level (25, 26).

Recently, lower vertebrates and invertebrates, such as *Caenorhabditis elegans*, *Drosophila melanogaster*, *Danio rerio*, and *Galleria mellonella*, became an attractive alternative to conventional murine models for studying host-pathogen interactions. They are used to examine the molecular mechanisms underlying the virulence strategies directed against the innate immune system and also to study the effectiveness of antimicrobial compounds *in vivo* (27). Among them are *G. mellonella* larvae, which exhibit immune defense mechanisms analogous to human innate responses, including both the cellular and the humoral components. There are at least eight types of hemocyte showing great similarity to the mammalian phagocytes that play a central role in antibacterial defense (28–30). The humoral response is achieved via the production of soluble effector molecules that immobilize or kill the pathogen. They include proteins homologous to the complement system, antibacterial peptides, and melanin (31, 32). The larvae can be used for subcutaneous injection, oral administration, and *in vivo* imaging (33, 34), for monitoring intracellular gene and protein expression (35–37), to detect immune responses (38), and to test antimicrobial drugs (39, 40). The use of this surrogate infectious model does not require special facilities; its short time and cost efficiency are significant benefits, and it does not raise ethical concerns. The lack of genetically modified strains of *G. mellonella* is a disadvantage, as the whole genome was described only in 2018 (41). Nevertheless, *G. mellonella* seems to be a very useful model for studying the corruption of innate immune mechanisms by pathogens.

The purpose of this study was to optimize two experimental models, *D. discoideum* and *G. mellonella*, in order to examine the virulence of *S. anginosus*. We found that *D. discoideum* can be used efficiently for large-scale screening of clinical isolates of *S. anginosus* with respect to their pathogenicity. To study the interactions between the bacteria and the host defense system and to explore the pathogenesis of *S. anginosus* infection, we used the *G. mellonella* model. We found during model development that *S. anginosus* strains varied in terms of their resistance to the bactericidal activity of phagocytes; therefore, the data obtained were verified using primary human neutrophils. Taken together, the data provide for the first time a set of models that can be used to investigate the mechanisms of *S. anginosus* pathogenesis.

RESULTS

Collection of *Streptococcus anginosus* isolates. For this study, we used a clinical collection of 23 *S. anginosus* isolates obtained from cases of severe (bacteremia [$n = 4$] and abscess [$n = 8$]) and mild (skin wounds [$n = 2$] and pharyngitis [$n = 9$]) infection. These strains were phenotypically characterized by examining the type of the Lancefield antigen, the type of hemolysis (alpha, beta, or gamma), DNase activity, and

TABLE 1 Phenotypic characterization of the clinical strains of *S. anginosus* used in the study

Strain	Source of isolate[a]	Lancefield antigen	Type of hemolysis	DNAse activity	Envelope
980/01	Blood	F	Gamma	+	Yes
4188/08	Pharyngitis	G	Beta	+	Yes
1658/06	Abscess	C	Alpha	−	Yes
4447/08	Abscess	G	Beta	+	Yes
4810/08	Pharyngitis	C	Alpha	+	Yes
2027/08	Abscess	A	Gamma	−	Yes
5652/09	Blood	C	Alpha	+	Yes
3114/96	Pharyngitis	C	Alpha	+	Yes
1834/01	Pharyngitis	C	Alpha	−	Yes
3027/03	Pharyngitis	C	Alpha	+	Yes
4020/05	Pharyngitis	F	Alpha	+	Yes
2087/07	Abscess	G	Alpha	+	Yes
2091/07	Pharyngitis	C	Alpha	+	Yes
2448/07	Skin wound	C	Alpha	+	Yes
2721/07	Skin wound	F	Gamma	−	Yes
3766/07	Abscess	C	Alpha	−	Yes
910/08	Blood	C	Alpha	+	Yes
4695/08	Pharyngitis	G	Beta	+	Yes
4737/08	Blood	No	Gamma	−	Yes
1505/09	Abscess	No	Gamma	−	Yes
1506/09	Abscess	No	Gamma	+	Yes
3792/10	Abscess	G	Beta	+	Yes
884/14	Pharyngitis	No	Beta	+	Yes

[a]Four strains were isolated from cases of bacteremia (blood), 8 from abscesses, 9 from cases of pharyngitis, and 2 from skin wounds.

the presence of the capsule [Table 1]. Given the different origins of the strains, as well as their varied phenotypes, we assumed that the bacterial collection was suitable to optimize and evaluate the models of virulence of *S. anginosus*.

***D. discoideum* as a model organism for large-scale screening of *S. anginosus* virulence.** To examine the ability of the collected *S. anginosus* strains to affect test organisms, we first focused on selecting a simple, low-cost, low-labor, and fast model. Therefore, we selected *D. discoideum* as a cellular model to study pathogen-phagocyte interactions, as such a simple screening model has never been described for *S. anginosus*. Therefore, we needed to optimize the whole procedure, from coculture of bacteria with amoebae to proper qualification and quantification of the interaction with the host. First, we optimized coculture of *D. discoideum* with *S. anginosus*. We found that the recommended conditions for *D. discoideum* growth (21°C, standard medium [SM] agar, and aerobic atmosphere) were inadequate for growing *S. anginosus*, because 52% of the tested *S. anginosus* isolates did not grow in the blood-free medium. Therefore, we modified the coculture conditions to enable the growth of *S. anginosus* without affecting the growth of *D. discoideum*. For this purpose, *D. discoideum* was seeded in SM medium with or without supplementation with 5% sheep blood, and plates were grown under the following four conditions: (I) 21°C, 20% oxygen atmosphere; (II) 21°C, microaerophilic atmosphere of 5% CO_2; (III) 37°C, 20% oxygen atmosphere; and (IV) 37°C, microaerophilic atmosphere of 5% CO_2 (Fig. 1A). The optimization process showed that culture at 37°C changed the morphology of *D. discoideum* colonies significantly, as they became jagged, fuzzy, and more transparent (Fig. 1A); thus, this temperature was eliminated for future experiments. The growth of *D. discoideum* at 21°C in blood-supplemented medium was more compact than that in SM medium. Under microaerophilic conditions, the growth of *D. discoideum* was slightly slower than the growth under aerobic conditions (Fig. 1A). Therefore, since the growth of *S. anginosus* was limited in the absence of a blood additive, we chose SM medium supplemented with 5% sheep blood, an oxygen atmosphere, and 21°C as our conditions for growth. Subsequently, we optimized *D. discoideum* infection with *S. anginosus* strain 980/01, which was isolated from cases of bacteriemia and classified as highly invasive. Infection was carried out at multiplicities of infection (MOIs) of 1:0.1 to 1:100 (Fig. 1B). The results showed that *D. discoideum* growth was

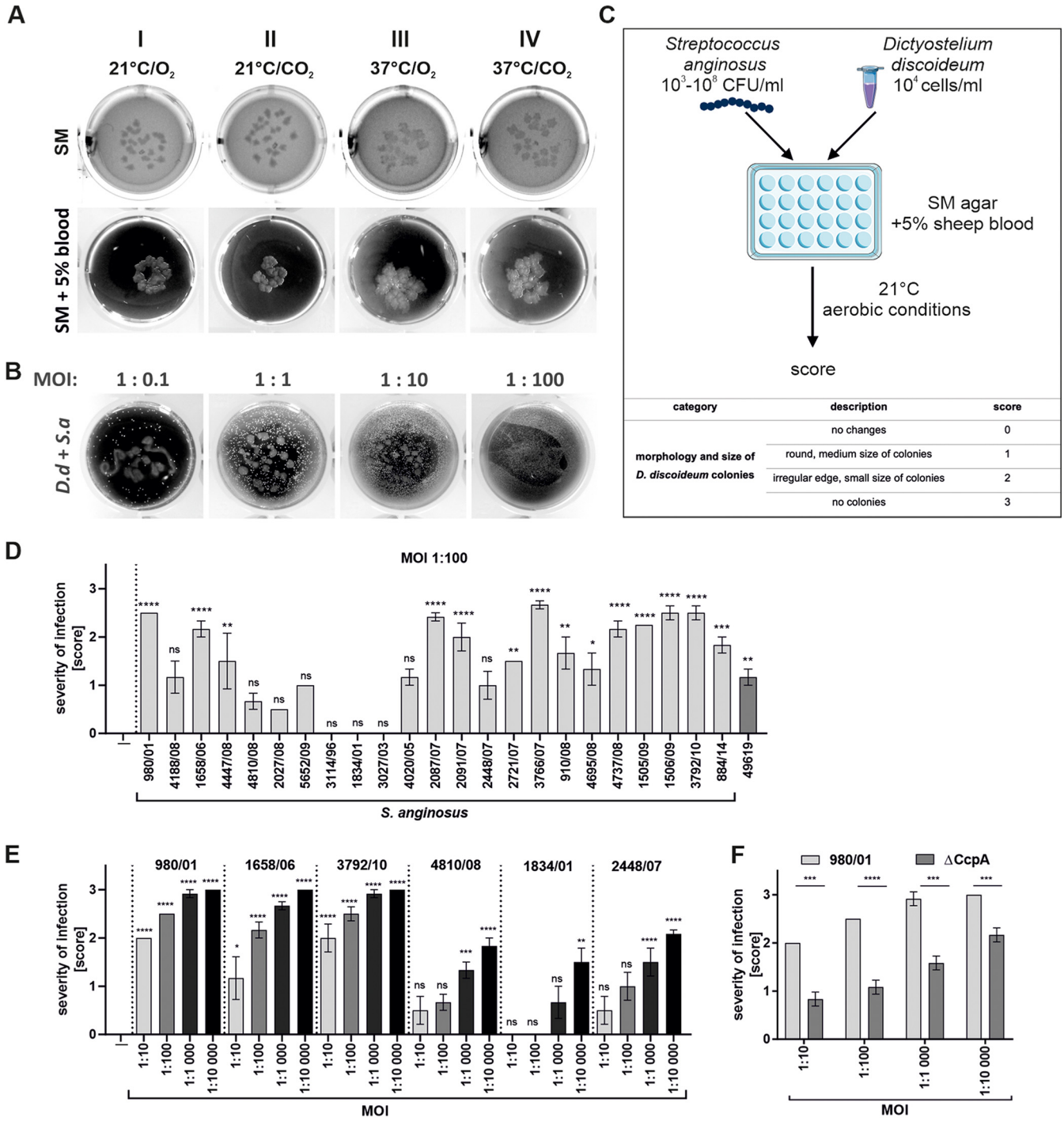

FIG 1 Infection of *D. discoideum* by *S. anginosus*. (A) Optimization of the growth conditions for *D. discoideum*. *D. discoideum* was seeded in SM and SM + 5% sheep blood medium at a density of 10^4 cells/mL. Growth was carried out for 4 days under the following conditions: (I) 20% oxygen atmosphere, 21°C (21°C/O_2); (II) 21°C, microaerophilic atmosphere enriched with CO_2 (21°C/CO_2); (III) 20% oxygen atmosphere, 37°C (37°C/O_2); and (IV) 37°C, microaerophilic atmosphere enriched with CO_2 (37°C/CO_2). (B) Representative photographs of *D. discoideum* growth inhibition after coculture with *S. anginosus* 980/01 at MOIs of 1:0.1 to 1:100. (C) Protocol for adoption of *D. discoideum* as a model for studying the virulence of *S. anginosus*. (D) Quantification of *D. discoideum* deterioration after *S. anginosus* infection. *S. anginosus* was seeded in SM medium along with *D. discoideum* at an MOI of 1:100. Cultures were monitored for 5 to 10 days. *D. discoideum* plated on SM medium in the absence of bacteria was used as a control. After 5 days of coculture at room temperature under aerobic conditions, *D. discoideum* growth was assessed and scored for the number and morphology of colonies. (E, F) Dose-dependent pathogenic effects of *S. anginosus* strains (E) and comparison of severities of infection caused by the WT (980/01) and the ΔCcpA mutant (980/01 ΔCcpA) (F). Data represent mean values from three independent experiments ± standard errors of the means (SEM). *, $P < 0.05$; **, $P < 0.01$; ***, $P < 0.001$; ****, $P < 0.0001$; ns, not significant.

inhibited efficiently by bacterial infection at an MOI of 1:10, with the most distinct effect observed at an MOI of 1:100 (Fig. 1B). The growth of *D. discoideum* was scored according to the number and morphology of the colonies compared with those from noninfected cultures of *D. discoideum*. A score of 0 describes typical and unaffected growth of amoebae, while a maximum score of 3 represents complete inhibition of growth by bacteria. As a positive control, we used *Streptococcus pneumoniae* ATCC 49619. Thus, we successfully used *D. discoideum* as a simple model to study the virulence of *S. anginosus*. The details of the newly developed protocol are presented in Fig. 1C. Next, we used the above-described protocol to examine the entire collection of *S. anginosus* strains in terms of virulence. *D. discoideum* was infected with bacteria at MOIs of 1:10 to 1:10 000 (Fig. 1D, Fig. S1), after which significant differences in strain-dependent pathogenicity were observed among the tested strains. Furthermore, we found that the pathogenic effect depended on the bacterial dose (Fig. 1E, Fig. S1). Finally, to confirm the suitability of the *D. discoideum* model for *S. anginosus* virulence studies, we examined the course of infection using an attenuated strain (generated in the *S. anginosus* 980/01 background) devoid of the catabolite control protein A (CcpA) (ΔCcpA mutant), which is a global regulator that controls the expression of many virulence factors in streptococci, including toxins (42). This mutation in other streptococci was used previously as a tool to demonstrate differences in virulence in various animal models (43–45). We found a significant reduction in the severity of *D. discoideum* infection using the mutated *S. anginosus* strain (Fig. 1F). The cumulative results indicate that *D. discoideum* is a useful model for fast and reliable large-scale screening of *S. anginosus* pathogenicity, as it allows discrimination of strains into high- and low-virulence tiers. However, it might not be sensitive enough to study minute differences in virulence.

***G. mellonella* as a model to study *S. anginosus*.** The experimental model based on *G. mellonella* has been used widely in recent years to study the mechanism underlying inactivation of innate immunity by pathogens like group A *streptococcus* (GAS), *Streptococcus suis*, and *Streptococcus pneumoniae* (46–50). However, *G. mellonella* has never been used to examine *S. anginosus*. Therefore, we decided to test whether the wax moth larva model could be used to study the strain-dependent pathogenicity of *S. anginosus* in more detail than the *D. discoideum* model. For this purpose, and in accordance with the results obtained from the *D. discoideum* model, we selected several strains of *S. anginosus* with various degrees of virulence (Fig. 1D). *G. mellonella* larvae were infected with one of the most (*S. anginosus* 980/01) and one of the least (*S. anginosus* 4810/08) virulent strains. *S. pneumoniae* ATCC 49619 was used as a positive control (48, 50). To determine the pathogenicity of *S. anginosus* in *G. mellonella*, a dose titration ranging from 1×10^6 to 1×10^8 CFU/larva was performed. Groups of 10 wax worms were infected through the last left proleg, with each larva receiving a single dose of *S. pneumoniae*, *S. anginosus*, or phosphate-buffered saline (PBS) (control). The highest pathogenic effect was observed in larvae infected with *S. anginosus* 980/01, which resulted in 100% mortality by 30 h postinfection (p.i.) at a dose of 1×10^8 CFU/larva (Fig. 2A). In particular, the mortality kinetics resembled the effects obtained after infection with *S. pneumoniae* ATCC 49619 (Fig. 2B). Infection with *S. anginosus* 4810/08 showed lower mortality, as 80% of the larvae survived up to 24 h p.i. (Fig. 2C). Quantification of the lethal dose (50% lethal dose [LD_{50}]) confirmed the significant differences in pathogenicity of the tested strains (Fig. 2D). Furthermore, wax worms were scored in terms of their melanization and activity (Fig. 2E to G). The data obtained revealed more severe symptoms in *G. mellonella* larvae infected with *S. anginosus* 980/01 (Fig. 2E) than in those infected with strain *S. anginosus* 4810/08 (Fig. 2G) at a dose of 1×10^7 CFU/larva. When the larvae were infected with a dose of 10^6 CFU, the severity of infection, estimated after 6 h, was significantly higher for strain 980/01 and *S. pneumoniae* than for strain 4810/08 (Fig. 2H). Furthermore, we found that the increase in the severity score and the decrease in survival were associated with the dose of bacteria. Next, we analyzed the pathogenic potential of the other *S. anginosus* strains in the collection. We found that strains isolated from cases of severe infection decreased larval survival (Fig. S2A) to a greater extent than isolates obtained from cases of mild infection (Fig. S2B). The ΔCcpA strain was used as a control infection. The data obtained showed a significant reduction in

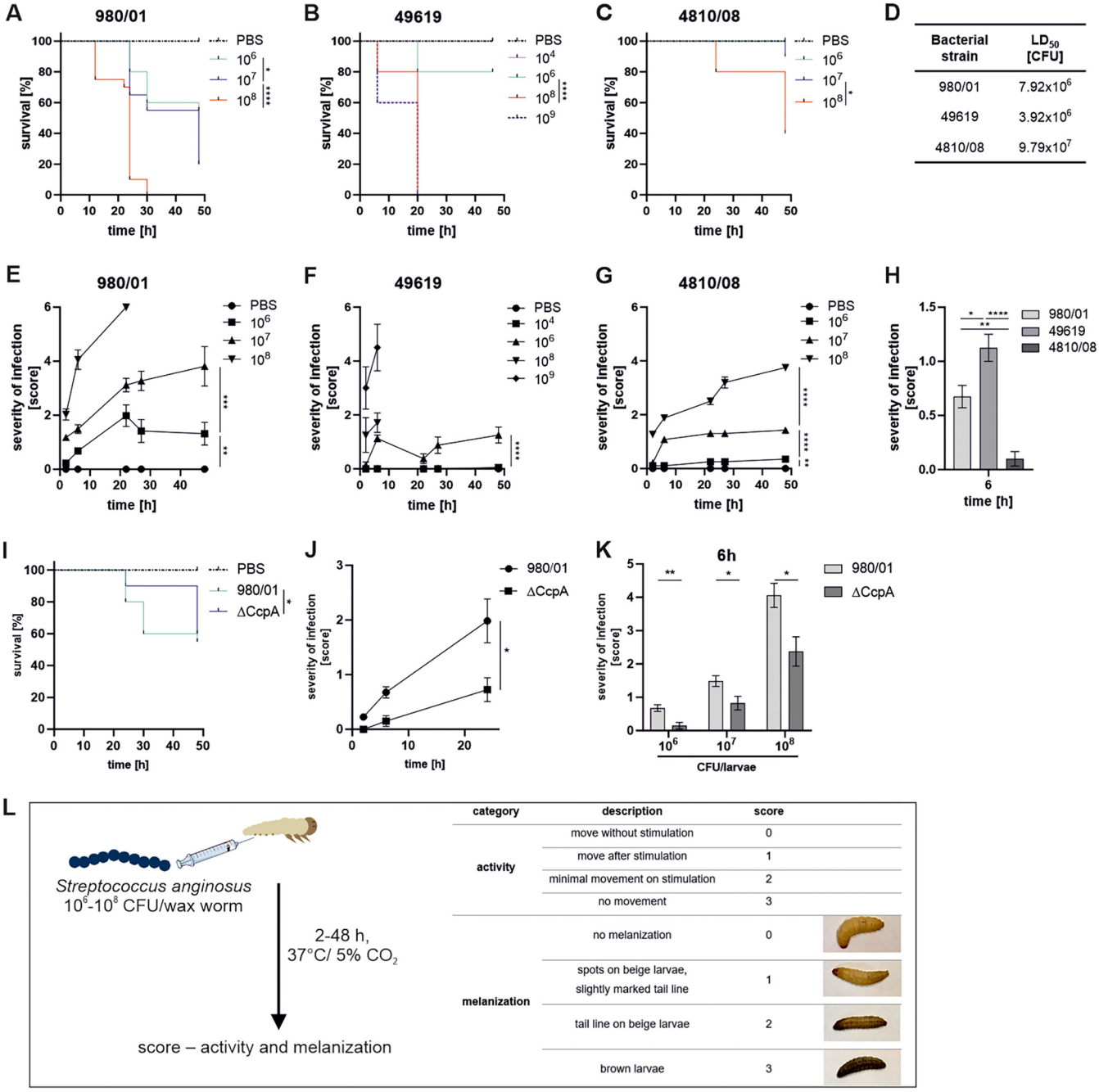

FIG 2 Virulence of *S. anginosus* and *S. pneumoniae* in *G. mellonella* larvae. Kaplan-Meier survival curves (A to C) and health index scores (E to G) of *G. mellonella* larvae after infection with different doses of *S. anginosus* and *S. pneumoniae*. The control group was injected with PBS. Each tested group contained 10 larvae (n = 10). (D) The LD_{50s} of *S. anginosus* and *S. pneumoniae* were calculated from a nonlinear regression analysis of larval death on day 2 p.i., with dose titration. Data are the mean values from two independent experiments. (H) Comparison of the degrees of severity of *S. anginosus* and *S. pneumoniae* infection at 6 h p.i. (10^6 CFU/larva). (I) Kaplan-Meier survival curves of *G. mellonella* larvae infected with *S. anginosus* 980/01 and/or 980/01ΔCcpA. (J) The severity of infection was scored for 980/01 and/or 980/01 ΔCcpA (10^6 CFU/larva). (K) The scores for larvae infected with different doses of 980/01 or 980/01 ΔCcpA were determined at 6 h p.i. (L) Protocol for adoption of *G. mellonella* larvae as a simple model for studying *S. anginosus* virulence. In all panels that include error bars, the data represent the mean values ± SEM. *, $P < 0.05$; **, $P < 0.01$; ***, $P < 0.001$; ****, $P < 0.0001$.

the mortality of larvae infected with the mutant strain compared to the mortality of larvae infected with the wild-type strain 980/01 (Fig. 2I). In particular, the severity of infection caused by 980/01 was significantly higher than that caused by the mutant (Fig. 2J) at 6 h p.i. and at all infectious doses tested (Fig. 2K). Thus, *G. mellonella* larvae are susceptible to infection by *S. anginosus*. The details of the newly developed protocol are presented in Fig. 2L.

***S. anginosus* survives, proliferates, and disseminates in the larvae of *Galleria mellonella*.** To identify factors that influence the deterioration of health status and mortality of *G. mellonella* larvae observed during *S. anginosus* infection, we examined the survival of bacteria in *G. mellonella* larvae. For that purpose, we applied a sublethal dose of *S. anginosus* (1×10^6 CFU/larva) and monitored the number of bacteria at 0.5, 3, 6, and 24 h p.i. At each time point, an individual larva was homogenized in PBS, and the liquid obtained was plated. We found that the number of highly virulent *S. anginosus* 980/01 bacteria recovered from the lysates increased over time (Fig. 3A), while the number of low-virulence *S. anginosus* 4810/08 bacteria decreased significantly (Fig. 3A). In particular, the estimated *in vitro* generation times in culture medium for both tested strains were comparable (Fig. 3B). To verify the above-described data, the hemolymph of infected larvae (1×10^6 CFU/larva) was isolated at 24 h p.i., cytospun, and stained with LIVE/DEAD stain to visualize bacteria. There was a higher number of live highly pathogenic *S. anginosus* 980/01 bacteria in hemolymph (Fig. 3C, green spots) than there was of low-virulence *S. anginosus* 4810/08 bacteria (Fig. 3C and D). Furthermore, Gram staining identified more aggressive dissemination of *S. anginosus* 980/01 to adjacent tissue, in contrast to the dissemination of strain 4810/08 (Fig. 3E). Taken together, these data indicate that highly virulent strains of *S. anginosus* are capable of growing and disseminating in a wax moth larva, likely because they are resistant to the host immune response.

Thus, we decided to examine the immune response of larvae to *S. anginosus* infection. Infection with *S. anginosus* 980/01 induced substantial increases in melanization and hemocyte infiltration, which were more intense than those observed for *S. anginosus* 4810/08 infection (Fig. 3F). Quantification of hemocytes in hemolymph collected at 24 h p.i. revealed their significant increase in *S. anginosus* 980/01 infected larvae compared to their number in noninfected and larvae infected with 4810/08 (Fig. 3G). To examine the activation of the defense system of *G. mellonella* after *S. anginosus* infection, we selected genes that play the most crucial role in immune defense and microbial clearance (51). Among them are genes encoding antimicrobial peptides (AMPs) (gallerimycin, galiomycin, gloverin, and cecropin) (52), hemolin, which acts as an opsonin (53), and a metalloproteinase inhibitor (IMPI) that protects the host from bacterial proteases (54), as well as *Hdd1*, which promotes the formation of nodules (55). We examined the expression of these molecules after infection with *S. anginosus*. For this purpose, larvae were infected with 10^6 CFU of 980/01 and/or 4810/08 strains, and RNA was collected at 6 and 24 h p.i. The expression of the gallerimycin, galiomycin, *Hdd11*, gloverin, cecropin, hemolin and IMPI genes was evaluated using quantitative reverse transcription-PCR (qRT-PCR) (Fig. 3H, Fig. S3). Of the studied transcripts, we observed a significant change only in *Hdd11* at 6 h p.i. (Fig. S3), the level of which increased by up to 3.5-fold after infection with both *S. anginosus* strains. In contrast to 4810/08, strain 980/01 induced a significant increase in all transcripts at 24 h p.i., except for IMPI gene transcripts (Fig. 3H). Thus, *S. anginosus* significantly promotes the mobilization of innate immune mechanisms but remains resistant to their bactericidal activity, which allows its efficient proliferation and dissemination in *G. mellonella* larvae. The data obtained indicate corruption of the host defense system by this pathogen.

Comparison of results from *S. anginosus* virulence models with those from a human phagocyte model. Next, we compared the degrees of virulence of *S. anginosus* isolates in both nonmammalian models and examined the clinical significance of infection. We found a significantly higher severity of infection for isolates from blood and deep tissue abscesses than for isolates from skin wounds and upper respiratory tract infections in both *D. discoideum* (Fig. 4A) and *G. mellonella* (Fig. 4B). Furthermore, we confirmed that the pathogenicity observed in *G. mellonella* was consistent with the results obtained for *D. discoideum*, as reflected by a positive Pearson correlation coefficient (0.6721) (Fig. 4C); this suggests compatibility of the two infection models tested. To provide stronger evidence that the results obtained using *D. discoideum* and *G. mellonella* reflect those in humans, we used a model based on primary human neutrophils. We selected these leukocytes as the main components of innate immunity because they

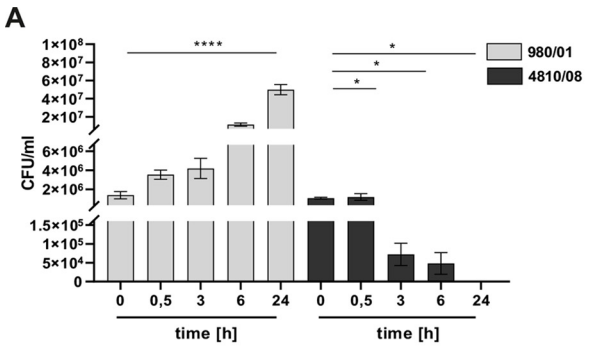

B

Bacterial strain	Generation time [h]
980/01	3.83 +/- 0.13
4810/08	3.80 +/- 0.08

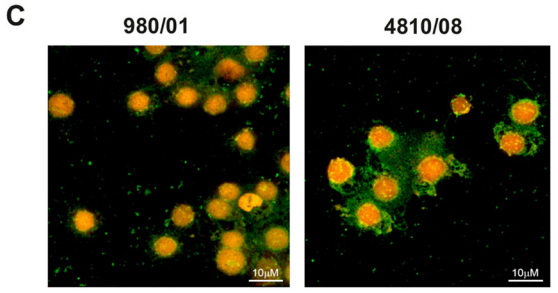

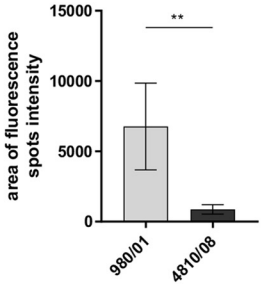

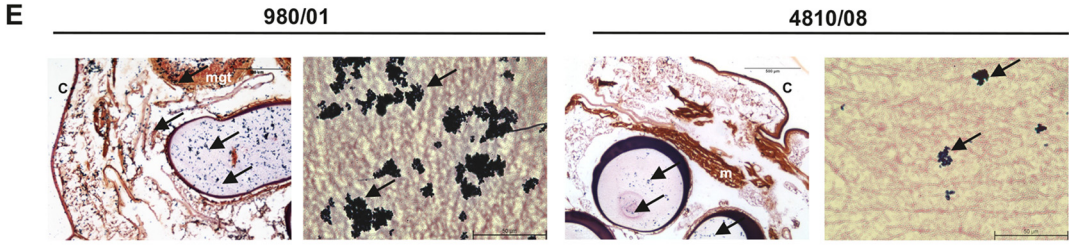

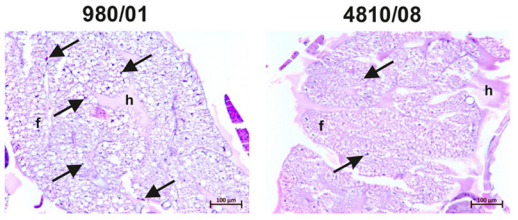

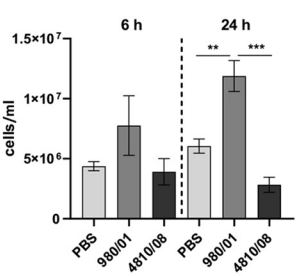

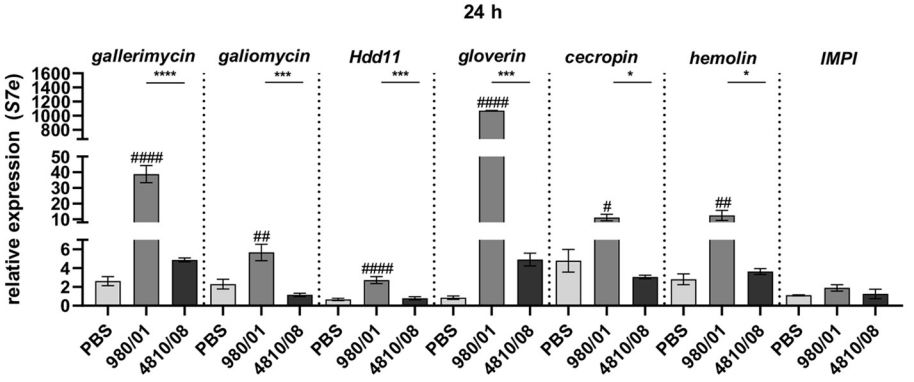

FIG 3 Survival of *S. anginosus* and activation of the innate immune response in *G. mellonella* larvae. (A) Larvae were infected with *S. anginosus* strains 980/01 and 4810/08 at a dose of 10^6 CFU/larva. At each time point, individual larvae were

(Continued on next page)

show phagocytic activity similar to those of *D. discoideum* (56, 57) and *G. mellonella* hemocytes (58). We then examined the bactericidal potential of neutrophils against selected strains ($n = 12$) from the collection. The data revealed that neutrophils significantly eradicated strains isolated from mild infections; however, strains isolated from bacteremia or abscesses were resistant (Fig. 4D). These results are consistent with the survival of bacteria in human blood (Fig. 4E). Collectively, the results indicate that the proposed models can be used to demonstrate the virulence potential of *S. anginosus*. Furthermore, our results suggest the pivotal role of phagocytes in defense against *S. anginosus*, which is reflected by the inactivation of bactericidal activity mediated by human neutrophils.

DISCUSSION

The pathogenic potential of *S. anginosus* was only noticed recently by clinicians as a consequence of improved microbiological diagnostic methods (59). Data regarding the virulence of these streptococci are limited, and we have almost no data that explain the molecular mechanisms used by these microorganisms during the infection process. To investigate bacterial pathogenesis, we need to rely on well-established models of infection. The models must allow discrimination between high- and low-virulence strains and, at the same time, trace interactions with the defense mechanisms of the host. Because the interaction between the pathogen and the intact host immune system cannot be traced in *in vitro* models, researchers must rely on animal models of infection. According to the 3R recommendations for animal experiments (reduction, replacement, and refinement), we wanted to establish and optimize a nonmammalian model or models that will allow us to efficiently and rapidly screen the virulence properties of *S. anginosus*, with a special focus on the innate immune system and its reaction to infection. We wanted to show the benefits, as well as the limitations, of experiments using alternative models to assess the virulence of *Streptococcus anginosus*. Therefore, we chose two nonmammalian organisms: *D. discoideum* and *G. mellonella*.

The key to understanding the mechanism of virulence is identification of the components of the immune response that are affected by pathogens. *Streptococcus anginosus* is often isolated from abscesses, suggesting that leukocyte accumulation in response to the infection process is insufficient to eliminate the invaders. The role of leukocytes in the pathogenicity of bacteria belonging to the *Streptococcus milleri* group (the former name for the *S. anginosus* group) was noted, and its reduced eradication by phagocytes was observed (60). However, the mechanism by which it avoids phagocytes remains unexplained at the molecular level. Therefore, we focused our initial study on the phagocyte model of *D. discoideum*. This soil-dwelling amoeba has been used as a host for many important pathogens, including *Vibrio cholerae* (13), *P. aerugi-*

FIG 3 Legend (Continued)
homogenized in 1 mL of PBS and the viability of the bacteria was estimated by counting CFU after plating on blood agar. Each test group contained 10 larvae ($n = 10$). Error bars show SEM. *, $P < 0.05$; **, $P < 0.01$; ***, $P < 0.001$; ****, $P < 0.0001$. (B) The generation time, *G*, was calculated using the equation $G = 0.301/a$, where *a* is the slope of the linear part of the growth curve plotted on a semilogarithmic scale. The experiments were carried out in triplicate. Data represent the mean values ± standard deviations (SD). (C, D) LIVE/DEAD staining of *S. anginosus* and *G. mellonella* hemocytes after infection. The larvae were infected with 10^6 CFU/larva. After 24 h, the larvae were sacrificed and the hemolymph was collected into a tube, seeded on polylysine slides, and stained with fluorescent LIVE/DEAD stain. (C) Viable cells of *S. anginosus* are stained green (SYTO 9), while red signals (propidium iodide [PI]) represent dead bacteria. Nuclear DNA from the host cells was stained with both SYTO 9 and PI. Scale bar = 10 μm. (D) Quantification of bacteria in the hemolymph of *G. mellonella*, calculated as the area of intensity of fluorescent spots from five different fields of view of the Z-stack. Error bars show SD. **, $P < 0.01$. (E) Gram-stained sections of *G. mellonella* larvae after *S. anginosus* infection (at 48 h p.i. with 10^6 CFU/larva). Arrows indicate bacteria around tubular organelles. c, cuticle; m, muscle; mgt, midgut tissues. (F) Histological analysis of larvae (at 48 h p.i. with 10^6 CFU/larva) was performed using hematoxylin-eosin staining (H&E). Arrows indicate areas of melanization. f, fat body; h, hemolymph. (G) Hemocytes of larvae (infected with bacteria at 10^6 CFU/larva) were extracted, and they were counted using a Fuchs-Rosenthal chamber. Error bars show SEM. **, $P < 0.01$; ***, $P < 0.001$. (H) qRT-PCR analysis of *G. mellonella* gene expression 24 h p.i. The larvae were frozen in liquid nitrogen and then lysed with TRIzol. RNA was isolated, and qRT-PCR was performed. Relative expression levels of the gallerimycin, galiomycin, *Hdd11*, gloverin, cecropin, hemolin, and IMPI genes are shown. The gene encoding ribosomal protein S7e (a housekeeping gene) was used for normalization. Data represent mean values from three independent experiments ± SEM. *P* values indicated by pound signs (#) are for comparisons to the control. #, $P < 0.05$; ##, $P < 0.01$; ###, $P < 0.001$; ####, $P < 0.0001$; *, $P < 0.05$; **, $P < 0.01$; ***, $P < 0.001$; ****, $P < 0.0001$.

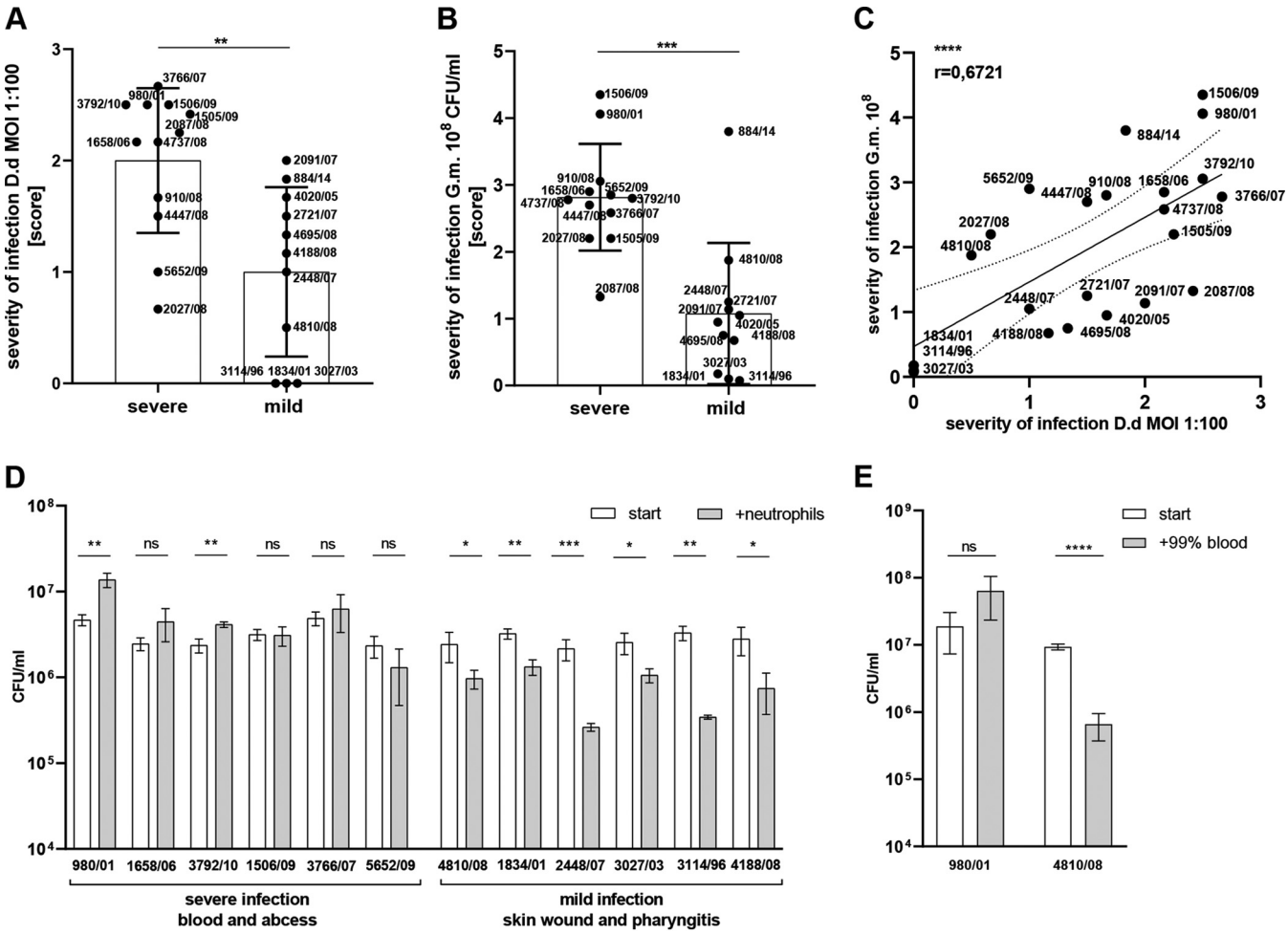

FIG 4 Comparison of the *D. discoideum*, *G. mellonella*, and human neutrophil models according to clinical severity of *S. anginosus* infection. (A, B) Comparison of the scores for severity of infection of *D. discoideum* (MOI of 1:100) (A) and *G. mellonella* (10^8 CFU/larva) (B) with *S. anginosus* strains isolated from severe and mild infections. Error bars show SEM. (C) Pearson's correlation analysis of the severity scores from the experiments whose results are shown in panels A and B. (D) Mean numbers of *S. anginosus* bacteria after a 90-min incubation with human neutrophils at an MOI of 1:5. After this time point, cells were lysed in 10% Triton X-100 and *S. anginosus* bacteria were counted after plating on blood agar. The experiments were carried out in duplicate. Data are presented as mean values ± SEM. (E) Killing of *S. anginosus* strains during incubation with whole blood. Suspensions of 10^7 CFU/mL of *S. anginosus* strains were added to 99% human blood. After 6 h, bacterial survival was investigated. Error bars show SD. *, $P < 0.05$; **, $P < 0.01$; ***, $P < 0.001$; ****, $P < 0.0001$; ns, not significant.

nosa (61), and *K. pneumoniae* (62); however, the application of *D. discoideum* to the study of streptococci has barely been described. The only report comes from Bonifait et al., who documented that *D. discoideum* could be used to examine the virulence of *S. suis* (20). In our study, we carefully optimized the method of infecting *D. discoideum* with *S. anginosus*, showing that it could be applied to large screening analyses. Moreover, our data indicate that *S. anginosus* develops efficient strategies against phagocytes. Among them could be limited pathogen recognition and reduced engulfment by phagocytes. We should also consider the release of factors that can inactivate bactericidal activity or lead to cytolysis of host cells. The pathogenic effect mediated by extracellular and/or released bacterial compounds was observed in our pilot studies (Fig. S4). Therefore, the role of leukocidins, antiopsonins, and/or nucleases is a potential direction for further research that could explain why strains from more severe infections evade neutrophil killing better. The hypothesis of inactivation of phagocytes as a virulence mechanism of *S. anginosus* is strongly supported by the observations made using *G. mellonella*. Interestingly, despite significant increases in the production of chemotactic agents (e.g., hemolin), and in the influx, accumulation, and aggregation of hemocytes, we observed survival and multiplication of *S.*

anginosus in vivo. It should be noted that there are many similarities between mammalian neutrophils and insect hemocytes (58). Insect hemocytes recognize pathogens and phagocytose them in a manner similar to that of neutrophils. Both human neutrophils and hemocytes have lectin-mediated phagocytosis and produce reactive oxygen species (ROS), extracellular traps, and antimicrobial peptides (AMPs). Additionally, both insect and human phagocytes possess the same receptors (e.g., Toll receptors), kinases (e.g., Jun N-terminal protein kinase [JNK]), and cascade pathways (e.g., JAK/STAT pathways). On the other hand, the molecular mechanisms used by *D. discoideum* to bind, ingest, and kill bacteria are analogous to those found in specialized phagocytic cells from multicellular organisms (56). Collectively, the inactivation of *D. discoideum* and of hemocytes of *G. mellonella* corroborates the resistance of *S. anginosus* to the bactericidal activity of human neutrophils, suggesting that these cells are the main target impaired by *S. anginosus* during infection. The above-described observation is of high importance and should be studied in more detail with the emphasis on the molecular mechanism underlying bacterial resistance to neutrophils.

The similarity of the innate response of *G. mellonella* larvae to that of mammalian systems allowed us to examine the mechanism through which humoral factors like AMPs work. *Galleria mellonella* produces a multitude of AMPs that are crucial for eliminating bacterial infection (30). Haine et al. proposed that these molecules play a more important role in counteracting persistent infection than in fighting acute infection (63). This could explain the delay in the expression of AMPs, except IMPI, that we documented 24 h after infection. The data obtained corroborate the observation made by Sheehan et al., who described an increase in gloverin and cecropin 24 h after infection with *S. aureus* (64). Furthermore, the increased expression of hemolin, a member of the immunoglobulin subfamily of recognition molecules (40), could help in the future to discriminate between lipoteichoic acids (LTAs) of *S. anginosus*, as the level of this protein depends on the LTA (65). These aspects could be investigated further, since putative regions encoding LTA have been identified in the *S. anginosus* genome, although their role in the pathogenesis of bacteria remains unknown (3).

G. mellonella seems to be a suitable model not only for studying the mechanisms underlying immune responses, but also for identifying the role of potential virulence factors. We documented this possibility by showing significant attenuation of strains devoid of CcpA. CcpA allows streptococci to absorb sugar from the environment, to colonize the oropharynx and nasopharynx, and to form biofilms (66–68). Furthermore, CcpA directly regulates the expression of toxins like streptolysin and intermedilysin by *Streptococcus pyogenes* and *S. intermedius*, respectively (42, 69, 70). Similarly, the application of the *G. mellonella* model to the *S. anginosus* study opens up the possibility of comparing *S. anginosus* with other streptococci, as in its previous use to examine *S. pneumoniae* (48, 50), *Streptococcus agalactiae* (71, 72), *S. pyogenes* (46, 47, 73, 74), and *Streptococcus mutans* (75, 76). A clear example is that our histological analysis revealed robust activation of immune defenses, which in some cases correlated with tissue damage, a common phenomenon associated with group A *streptococcus* infection (47). In addition to cytolysin genes, numerous putative genes that encode proteases have been identified in the genome of *S. anginosus* (3); thus, the role of these enzymes in disseminating bacteria from the hemolymph should be studied in the future.

The main limitation of using *D. discoideum* is temperature, as according to the optimized method, the experiments should be carried out at 21°C. Streptococci, including GAS (77), *S. agalactiae* (78), and *S. pneumoniae* (79), change their transcriptome profiles significantly when growing at temperatures lower than 37°C. GAS manifest significant decreases in hemolytic and nuclease activities when grown at 30°C. In contrast, some genes, mainly those involved in metabolism, replication, and recombination and in DNA repair, transport, and binding, are upregulated at lower temperatures (77). Therefore, *S. anginosus* growth and gene expression should be evaluated at the temperature used in the *D. discoideum*

model when the molecular mechanism of the observed interaction is studied. This aspect can be omitted from the *G. mellonella* model, as it can be handled at a physiological mammalian temperature of 37°C (80, 81), giving it an apparent advantage over other invertebrate model hosts, such as *Caenorhabditis elegans* and *Drosophila melanogaster* (82). It should be noted that, as the *G. mellonella* genome has been described (41), we also have the possibility of genetic manipulation of the host. Furthermore, although we have not examined it for this, we propose that *G. mellonella* would be a suitable model for studying the efficacy of therapeutic agents *in vivo*, as described for other streptococci (50).

In conclusion, we show that *D. discoideum* and *G. mellonella* are suitable models for studying the pathogenicity of *S. anginosus*. The main advantage of the sequential application of both models presented herein is the ease of establishment and maintenance, the low cost, and the feasibility of high-throughput studies (72). The results obtained for both models are comparable, they corroborate clinical data, and the model based on human leukocytes allows the reliable selection of strains with extremely high or extremely low virulence.

MATERIALS AND METHODS

Bacterial strains. *S. anginosus* strains were obtained from National Medicines Institute, Warsaw, Poland (83), while the *Streptococcus pneumoniae* control strain (ATCC 49619) was purchased from ATCC. Streptococci were grown in tryptic soy broth (TSB; Sigma-Aldrich) liquid medium at 37°C under microaerophilic conditions with 5% CO_2. Bacterial cells were collected by centrifugation after overnight culture (5,000 $\times$ *g* for 5 min at 20°C), washed twice with PBS (Dulbecco's phosphate-buffered saline without Ca^{2+} and Mg^{2+}), and resuspended in PBS to an optical density of 1.0 measured at 600 nm (OD_{600}), which corresponds to 1 $\times$ 10^8 CFU per mL (CFU/mL).

Construction of ΔCcpA strain. The mutant construction (980/01 ΔCcpA) was performed in a manner analogous to the previously described construction of a Δ*codY* mutant (84). Primers were designed for the sequences upstream and downstream from both flanks of the *ccp*A gene (*ccpA* Left flank Forward, CTGTCCGTGTCATATCGCTGGCATAACC, and Left flank Reverse GTTATAGTTATTATAACATGTATT CCCGGGGCATGCTTCTTCCTTTCTATATTGAAAATATCGTTTTCACATTC; *ccpA* Right flank Forward, TTAAATAA CAGATTAAAAAAATTATAACCCGGGTAAGTAGAGTTAGACAGAACTTGAAATTTTCAATTTTAAG, and Right flank Reverse GCACCACAATCCCTTCTGTTTCTTCATAACTG) and for the spectinomycin resistance gene from plasmid pSL60 (85) (*spc* forward CCCGGGAATACATGTTATAATAACTATAACTAAT, and *spc* reverse, CCCGGGTTA TAATTTTTTTAATCTGTTATTT).

Phenotypic characterization of *S. anginosus* strains. The Lancefield antigen detection was performed using the streptococcal grouping kit (Oxoid) according to the manufacturer's instructions. Qualitative determination of hemolysis was performed after 24 h of bacterial growth in Columbia agar medium (Sigma-Aldrich) with 5% sheep blood. The appearance of a clear zone surrounding the colony was classified as beta-hemolysis, while a greenish zone was classified as alpha-hemolysis and no zone was designated as gamma-hemolysis. DNase activity was examined by plating bacteria on BD DNase test agar plates. Plates were incubated at 37°C under microaerophilic conditions with 5% CO_2 for 24 h. After incubation, 1 M HCl was poured onto the plate and incubated for at least 2 min. On the basis of the presence of a clear zone around the bacteria, the ability to produce DNases was determined. The presence of a cell capsule was estimated by negative dyeing with India ink and visualization under a light microscope.

Growth properties of *S. anginosus* strains. *S. anginosus* strains were transferred from plates with Columbia agar with 5% sheep blood to a TSB medium and grown at 37°C under microaerophilic conditions with 5% CO_2. After overnight culture, bacteria were used to inoculate new cultures at an OD_{600} of 0.15 in duplicates and grown under the same conditions. The optical density of the culture was measured at a wavelength of 600 nm every 2 h for 10 h. Generation times, *G*, were calculated with the equation $G = 0.301/a$, where *a* is the slope of the linear part of the growth curve.

Culture of *D. discoideum*. *D. discoideum* ATCC 28368 was grown in glass flasks with liquid medium HL-5 supplemented with glucose, vitamins and microelements (Formedium, England - cat# HLE1) (14 g/L peptone, 7 g/L yeast extract, 13.5 g/L glucose, 0.5 g/L KH_2PO_4, 0.5 g/L Na_2HPO_4, 0.01 g/L FM vitamins, and microelements) at 21°C with shaking (180 rpm) until used for experiments. Cell density was monitored by cell counting using a Fuchs-Rosenthal chamber. Cell density in culture did not exceed 10^7 cells/mL. For infection studies, cells were counted and diluted to a density of 10^4 cells/mL and seeded in solid medium. The culture method was optimized as described in Results.

Bacterial virulence assay with *D. discoideum*. Overnight cultures of *S. anginosus* or control strains were diluted in PBS to the desired serial densities of 10^3 to 10^8 CFU/mL. Fifty microliters of each *S. anginosus* dilution or control strain was deposited in a well of a 24-well plate filled with 2 mL of 5% sheep blood SM agar (10 g/L peptone, 1 g/L yeast extract, 10 g/L glucose, 1.9 g/L KH_2PO_4, 1.3 g/L K_2HPO_4 $3H_2O$, 0.49 g/L anhydrous $MgSO_4$, 16 g/L agar). When the surface of the well was dry, five μL of HL-5 medium containing 10^4 cells/mL of *D. discoideum* was added to the bacterial lawn and the plate was incubated at 21°C.

To discriminate the effect of bacterial phagocytosis from the activity of secreted bacterial compounds, *D. discoideum* was incubated with 5 μM cytochalasin D for 30 min at room temperature before

being added to the bacterial lawn (86). The growth of *D. discoideum* with *S. anginosus* was monitored for 5 to 10 days. After 5 days of coculture, the inhibition of *D. discoideum* growth was scored for the number and morphology of *D. discoideum* colonies and compared to the growth of *D. discoideum* seeded alone. The score representing typical, unaffected growth of *D. discoideum* was set at 0, and changes in morphology were addressed as presented in Fig. 1. If necessary, intermediate values were used.

***G. mellonella* infection model.** The *G. mellonella* larvae were purchased from Biosystems Technology and stored in the dark at 17°C. Only healthy larvae with no signs of melanization were used in the experiments. Ten larvae per group were infected by injection into the last proleg using a Hamilton syringe with 10 μL of bacterial inoculum containing from 10^5 to 10^8 CFU of *S. anginosus*. Ten microliters of PBS was used as a control. The larvae were incubated at 37°C in 9-cm Petri dishes without food. Their condition in terms of activity and melanization was monitored up to 48 h after infection and scored as presented in Fig. 2. The larvae were considered dead when they did not move in response to tactile stimulation.

Isolation of the hemolymph of *G. mellonella*. To collect larval hemolymph, larvae were wiped with 70% ethanol and then an incision was made on the proleg with a scalpel. Five microliters of hemolymph was mixed with the same volume of ice-cold PBS buffer with 0.36% β-mercaptoethanol to prevent coagulation and melanization and immediately used for the quantification of the number of hemocytes by trypan blue staining.

Bacterial viability in the hemolymph of *G. mellonella*. The survival of bacteria in hemolymph was examined using the LIVE/DEAD BacLight kit (Molecular Probes). The hemolymph was collected as described above and cytospun on polylysine glass. The staining procedure was performed according to the manufacturer's instructions. Bacteria were visualized by confocal laser scanning microscopy (CLSM) using a Zeiss LSM 880 confocal system equipped with 100× oil immersion objectives. The acquired Z-stack images from five different fields of view were analyzed using Zeiss ZEN microscopy software and Fiji software. The quantification of bacteria in the hemolymph of *G. mellonella* was calculated as an area of fluorescence spot intensity using ImageJ software.

Bacterial survival/proliferation in *G. mellonella* larvae. At different time points postinfection (p.i.) of *G. mellonella* larvae with *S. anginosus*, larvae were homogenized in 1 mL of PBS by mechanical force. The samples were serially diluted in PBS and plated on Columbia agar with 5% sheep blood, and colonies were counted after incubation at 37°C for 48 h. As a control, PBS-injected larvae were used in an analogous procedure.

Histopathological analysis of *G. mellonella* specimens. Larvae injected with 10 μL of PBS (control) or 10^6 CFU of *S. anginosus* were sacrificed by freezing 48 h after injection. The larvae were then injected with 100 μL of 10% formalin to fix internal organs and then stored for 24 h at 4°C. The larvae were cut along segments and embedded into wax blocks. Tissue sections (10 μm) were stained with hematoxylin-eosin or Gram stain. Sections were examined using a light microscope.

RNA isolation and qRT-PCR. Six and 24 h after infection, larvae infected with 10^6 CFU of *S. anginosus* were snap-frozen in liquid nitrogen and homogenized. Then, TRI Reagent (Sigma-Aldrich) was used to extract RNA according to the manufacturer's instructions. Reverse transcription was performed using the high-capacity cDNA reverse transcription kit (Applied Biosystems). One microgram of RNA from each sample was used for cDNA synthesis with oligo(dT) primers according to the manufacturer's instructions. Quantitative reverse transcription-PCR (qRT-PCR) was performed with the SYBR green method in a reaction mixture volume of 15 μL, containing 0.5 μL of cDNA sample, 10 μM forward and reverse primers, and 1× GoTaq qPCR master mix (Promega). The primers and conditions for denaturation, annealing, and extension for each pair of primers are listed in Table S1 (53, 65, 87, 88).

The qRT-PCR was initiated by denaturation for 3 min, and the amplification program was carried out for 44 cycles with a final elongation step at 72°C for 10 min.

The gene encoding ribosomal protein S7e, a housekeeping gene, was used for normalization. The means of the threshold cycle (C_T) values were calculated and analyzed using the $\Delta\Delta C_T$ quantification method (89). To verify the specificity of quantitative PCR (qPCR) products, melt curve analyses were performed.

Isolation of human neutrophils. Blood was purchased from the Regional Blood Center, Krakow, Poland. It was collected from healthy donors who provided written informed consent for the collection of samples and subsequent cell isolation and analysis. For human subject confidentiality assurances, blood material was de-identified; thus, this study adheres to appropriate exclusions from human subject approval. Neutrophils were isolated from fractions of peripheral blood enriched with granulocytes, which were harvested using a density gradient. Neutrophils and erythrocytes were collected as the high-density fraction. To separate neutrophils from erythrocytes, this fraction was incubated for 30 min with 1% polyvinyl alcohol (POCH; Poland). Neutrophils were collected from the upper layer. After centrifugation (280 × *g* for 10 min at 20°C), other erythrocytes were removed by lysis in water. Neutrophils were resuspended in serum-free Dulbecco modified Eagle medium (DMEM) without phenol red (Gibco/ThermoFisher Scientific, USA).

PMN killing assay. A suspension of *S. anginosus* in DMEM (without phenol red) with 1% autological human serum was added to 5×10^5 polymorphonuclear leukocytes (PMN)/well seeded in DMEM in 96-well plates at an MOI of 1:5 (cells-to-bacteria ratio), and the plates were centrifuged (300 × *g* for 8 min at 20°C). PMN and *S. anginosus* were cocultured for 90 min in a humidified atmosphere containing 5% CO_2. After 90 min, cells were lysed by adding 20 μL of 10% Triton X-100. The samples were serially diluted in PBS and seeded in Columbia agar with 5% sheep blood, and colonies were counted after incubation at 37°C for 48 h.

Whole-blood killing. A suspension of 10^7 CFU/mL of *S. anginosus* was added to human blood. The samples were incubated for 6 h at 37°C. After 6 h, samples were serially diluted in PBS and plated on Columbia agar with 5% sheep blood, and colonies were counted after incubation at 37°C for 48 h.

Statistical analysis. Data were analyzed using GraphPad Prism version 9.1.1 (GraphPad Software). Parametric tests (unpaired Student's *t* test or analysis of variance [ANOVA] and Pearson correlation coefficients) were used. A *P* value of <0.05 was used for statistical significance. The logarithmic rank test (Mantel-Cox) was used for survival analyses.

SUPPLEMENTAL MATERIAL

Supplemental material is available online only.

SUPPLEMENTAL FILE 1, PDF file, 0.7 MB.

ACKNOWLEDGMENTS

The study was funded by National Science Center, Poland, grant no. 2018/29/B/NZ6/00624. The funders had no role in study design, data collection, and analysis, decision to publish, or preparation of the manuscript.

All authors declared that they have no conflict of interest to disclose.

REFERENCES

1. Pilarczyk-Zurek M, Sitkiewicz I, Koziel J. 2022. The clinical view on Streptococcus anginosus group—opportunistic pathogens coming out of hiding. Front Microbiol 13:2533. https://doi.org/10.3389/fmicb.2022.956677.
2. Suzuki H, Hase R, Otsuka Y, Hosokawa N. 2016. Bloodstream infections caused by Streptococcus anginosus group bacteria: a retrospective analysis of 78 cases at a Japanese tertiary hospital. J Infect Chemother 22:456–460. https://doi.org/10.1016/j.jiac.2016.03.017.
3. Sitkiewicz I. 2018. How to become a killer, or is it all accidental? Virulence strategies in oral streptococci. Mol Oral Microbiol 33:1–12. https://doi.org/10.1111/omi.12192.
4. Asam D, Mauerer S, Spellerberg B. 2015. Streptolysin S of Streptococcus anginosus exhibits broad-range hemolytic activity. Med Microbiol Immunol 204:227–237. https://doi.org/10.1007/s00430-014-0363-0.
5. Asam D, Spellerberg B. 2014. Molecular pathogenicity of Streptococcus anginosus. Mol Oral Microbiol 29:145–155. https://doi.org/10.1111/omi.12056.
6. Babbar A, Kumar VN, Bergmann R, Barrantes I, Pieper DH, Itzek A, Nitsche-Schmitz DP. 2017. Members of a new subgroup of Streptococcus anginosus harbor virulence related genes previously observed in Streptococcus pyogenes. Int J Med Microbiol 307:174–181. https://doi.org/10.1016/j.ijmm.2017.02.002.
7. Tsunashima H, Miyake K, Motono M, Iijima S. 2012. Organization of the capsule biosynthesis gene locus of the oral streptococcus Streptococcus anginosus. J Biosci Bioeng 113:271–278. https://doi.org/10.1016/j.jbiosc.2011.10.013.
8. Barnett TC, Cole JN, Rivera-Hernandez T, Henningham A, Paton JC, Nizet V, Walker MJ. 2015. Streptococcal toxins: role in pathogenesis and disease. Cell Microbiol 17:1721–1741. https://doi.org/10.1111/cmi.12531.
9. Nobbs AH, Lamont RJ, Jenkinson HF. 2009. Streptococcus adherence and colonization. Microbiol Mol Biol Rev 73:407–450. https://doi.org/10.1128/MMBR.00014-09.
10. Homer KA, Denbow L, Whiley RA, Beighton D. 1993. Chondroitin sulfate depolymerase and hyaluronidase activities of viridans streptococci determined by a sensitive spectrophotometric assay. J Clin Microbiol 31:1648–1651. https://doi.org/10.1128/jcm.31.6.1648-1651.1993.
11. Jacobs JA, Schot CS, Schouls LM. 2000. Haemolytic activity of the 'Streptococcus milleri group' and relationship between haemolysis restricted to human red blood cells and pathogenicity in S. intermedius. J Med Microbiol 49:55–62. https://doi.org/10.1099/0022-1317-49-1-55.
12. Kanamori S, Kusano N, Shinzato T, Saito A. 2004. The role of the capsule of the Streptococcus milleri group in its pathogenicity. J Infect Chemother 10:105–109. https://doi.org/10.1007/s10156-004-0305-7.
13. Pukatzki S, Ma AT, Sturtevant D, Krastins B, Sarracino D, Nelson WC, Heidelberg JF, Mekalanos JJ. 2006. Identification of a conserved bacterial protein secretion system in Vibrio cholerae using the Dictyostelium host model system. Proc Natl Acad Sci U S A 103:1528–1533. https://doi.org/10.1073/pnas.0510322103.
14. Froquet R, Cherix N, Burr SE, Frey J, Vilches S, Tomas JM, Cosson P. 2007. Alternative host model to evaluate Aeromonas virulence. Appl Environ Microbiol 73:5657–5659. https://doi.org/10.1128/AEM.00908-07.
15. Cosson P, Zulianello L, Join-Lambert O, Faurisson F, Gebbie L, Benghezal M, Van Delden C, Kocjancic Curty L, Köhler T. 2002. Pseudomonas aeruginosa virulence analyzed in a Dictyostelium discoideum host system. J Bacteriol 184:3027–3033. https://doi.org/10.1128/JB.184.11.3027-3033.2002.
16. Alibaud L, Köhler T, Coudray A, Prigent-Combaret C, Bergeret E, Perrin J, Benghezal M, Reimmann C, Gauthier Y, Van Delden C, Attree I, Fauvarque MO, Cosson P. 2008. Pseudomonas aeruginosa virulence genes identified in a Dictyostelium host model. Cell Microbiol 10:729–740. https://doi.org/10.1111/j.1462-5822.2007.01080.x.
17. Aubert DF, Flannagan RS, Valvano MA. 2008. A novel sensor kinase-response regulator hybrid controls biofilm formation and type VI secretion system activity in Burkholderia cenocepacia. Infect Immun 76:1979–1991. https://doi.org/10.1128/IAI.01338-07.
18. Hasselbring BM, Patel MK, Schell MA. 2011. Dictyostelium discoideum as a model system for identification of Burkholderia pseudomallei virulence factors. Infect Immun 79:2079–2088. https://doi.org/10.1128/IAI.01233-10.
19. Alibaud L, Rombouts Y, Trivelli X, Burguière A, Cirillo SLG, Cirillo JD, Dubremetz JF, Guérardel Y, Lutfalla G, Kremer L. 2011. A Mycobacterium marinum TesA mutant defective for major cell wall-associated lipids is highly attenuated in Dictyostelium discoideum and zebrafish embryos. Mol Microbiol 80:919–934. https://doi.org/10.1111/j.1365-2958.2011.07618.x.
20. Bonifait L, Charette SJ, Filion G, Gottschalk M, Grenier D. 2011. Amoeba host model for evaluation of Streptococcus suis virulence. Appl Environ Microbiol 77:6271–6273. https://doi.org/10.1128/AEM.00659-11.
21. Dunn JD, Bosmani C, Barisch C, Raykov L, Lefrançois LH, Cardenal-Muñoz E, López-Jiménez AT, Soldati T. 2017. Eat prey, live: Dictyostelium discoideum as a model for cell-autonomous defenses. Front Immunol 8:1906. https://doi.org/10.3389/fimmu.2017.01906.
22. Koller B, Schramm C, Siebert S, Triebel J, Deland E, Pfefferkorn AM, Rickerts V, Thewes S. 2016. Dictyostelium discoideum as a novel host system to study the interaction between phagocytes and yeasts. Front Microbiol 7:1665. https://doi.org/10.3389/fmicb.2016.01665.
23. Kjellin J, Pränting M, Bach F, Vaid R, Edelbroek B, Li Z, Hoeppner MP, Grabherr M, Isberg RR, Hagedorn M, Söderbom F. 2019. Investigation of the host transcriptional response to intracellular bacterial infection using Dictyostelium discoideum as a host model. BMC Genomics 20:1–18. https://doi.org/10.1186/s12864-019-6269-x.
24. González-Velasco Ó, de Las Rivas J, Lacal J. 2019. Proteomic and transcriptomic profiling identifies early developmentally regulated proteins in Dictyostelium discoideum. Cells 8:1187. https://doi.org/10.3390/cells8101187.
25. Gruenheit N, Baldwin A, Stewart B, Jaques S, Keller T, Parkinson K, Salvidge W, Baines R, Brimson C, Wolf JB, Chisholm R, Harwood AJ, Thompson CRL. 2021. Mutant resources for functional genomics in Dictyostelium discoideum using REMI-seq technology. BMC Biol 19:1–19. https://doi.org/10.1186/s12915-021-01108-y.

26. Lampe EO, Brenz Y, Herrmann L, Repnik U, Griffiths G, Zingmark C, Sjöstedt A, Winther-Larsen HC, Hagedorn M. 2015. Dissection of Francisella host cell interactions in Dictyostelium discoideum. Appl Environ Microbiol 82:1586–1598. https://doi.org/10.1128/AEM.02950-15.
27. Glavis-Bloom J, Muhammed M, Mylonakis E. 2012. Of model hosts and man: using Caenorhabditis elegans, Drosophila melanogaster and Galleria mellonella as model hosts for infectious disease research. Adv Exp Med Biol 710:11–17. https://doi.org/10.1007/978-1-4419-5638-5_2.
28. Tojo S, Naganuma F, Arakawa K, Yokoo S. 2000. Involvement of both granular cells and plasmatocytes in phagocytic reactions in the greater wax moth, Galleria mellonella. J Insect Physiol 46:1129–1135. https://doi.org/10.1016/s0022-1910(99)00223-1.
29. Altincicek B, Stötzel S, Wygrecka M, Preissner KT, Vilcinskas A. 2008. Host-derived extracellular nucleic acids enhance innate immune responses, induce coagulation, and prolong survival upon infection in insects. J Immunol 181:2705–2712. https://doi.org/10.4049/jimmunol.181.4.2705.
30. Tsai CJY, Loh JMS, Proft T. 2016. Galleria mellonella infection models for the study of bacterial diseases and for antimicrobial drug testing. Virulence 7:214–229. https://doi.org/10.1080/21505594.2015.1135289.
31. Hoffmann JA. 1995. Innate immunity of insects. Curr Opin Immunol 7:4–10. https://doi.org/10.1016/0952-7915(95)80022-0.
32. Lionakis MS. 2011. Drosophila and Galleria insect model hosts: new tools for the study of fungal virulence, pharmacology and immunology. Virulence 2:521–527. https://doi.org/10.4161/viru.2.6.18520.
33. Sänger PA, Wagner S, Liebler-Tenorio E, Fuchs TM. 2022. Dissecting the invasion of Galleria mellonella by Yersinia enterocolitica reveals metabolic adaptations and a role of a phage lysis cassette in insect killing. PLoS Pathog 18:e1010991. https://doi.org/10.1371/journal.ppat.1010991.
34. Quansah E, Ramoji A, Thieme L, Mirza K, Goering B, Makarewicz O, Heutelbeck A, Meyer-Zedler T, Pletz MW, Schmitt M, Popp J. 2022. Label-free multimodal imaging of infected Galleria mellonella larvae. Sci Rep 12:1–14. https://doi.org/10.1038/s41598-022-24846-7.
35. Zhao HX, Xiao WY, Ji CH, Ren Q, Xia XS, Zhang XF, Huang WZ. 2019. Candidate chemosensory genes identified from the greater wax moth, Galleria mellonella, through a transcriptomic analysis. Sci Rep 9:10032. https://doi.org/10.1038/s41598-019-46532-x.
36. Sheehan G, Clarke G, Kavanagh K. 2018. Characterisation of the cellular and proteomic response of Galleria mellonella larvae to the development of invasive aspergillosis. BMC Microbiol 18:1–11. https://doi.org/10.1186/s12866-018-1208-6.
37. Paulson AR, O'Callaghan M, Zhang XX, Rainey PB, Hurst MRH. 2021. In vivo transcriptome analysis provides insights into host-dependent expression of virulence factors by Yersinia entomophaga MH96, during infection of Galleria mellonella. G3 (Bethesda) 11:jkaa024. https://doi.org/10.1093/g3journal/jkaa024.
38. Vertyporokh L, Wojda I. 2020. Immune response of Galleria mellonella after injection with non-lethal and lethal dosages of Candida albicans. J Invertebr Pathol 170:107327. https://doi.org/10.1016/j.jip.2020.107327.
39. Nowicki D, Krause K, Karczewska M, Szalewska-Pałasz A. 2021. Evaluation of the anti-shigellosis activity of dietary isothiocyanates in Galleria mellonella larvae. Nutrients 13:3967. https://doi.org/10.3390/nu13113967.
40. Benthall G, Touzel RE, Hind CK, Titball RW, Sutton JM, Thomas RJ, Wand ME. 2015. Evaluation of antibiotic efficacy against infections caused by planktonic or biofilm cultures of Pseudomonas aeruginosa and Klebsiella pneumoniae in Galleria mellonella. Int J Antimicrob Agents 46:538–545. https://doi.org/10.1016/j.ijantimicag.2015.07.014.
41. Lange A, Beier S, Huson DH, Parusel R, Iglauer F, Frick JS. 2018. Genome sequence of Galleria mellonella (greater wax moth). Genome Announc 6:e01220-17. https://doi.org/10.1128/genomeA.01220-17.
42. Tomoyasu T, Tabata A, Hiroshima R, Imaki H, Masuda S, Whiley RA, Aduse-Opoku J, Kikuchi K, Hiramatsu K, Nagamune H. 2010. Role of catabolite control protein A in the regulation of intermedilysin production by Streptococcus intermedius. Infect Immun 78:4012–4021. https://doi.org/10.1128/IAI.00113-10.
43. Shelburne SA, Olsen RJ, Suber B, Sahasrabhojane P, Sumby P, Brennan RG, Musser JM. 2010. A combination of independent transcriptional regulators shapes bacterial virulence gene expression during infection. PLoS Pathog 6:e1000817. https://doi.org/10.1371/journal.ppat.1000817.
44. Watson ME, Nielsen HV, Hultgren SJ, Caparon MG. 2013. Murine vaginal colonization model for investigating asymptomatic mucosal carriage of Streptococcus pyogenes. Infect Immun 81:1606–1617. https://doi.org/10.1128/IAI.00021-13.
45. Paluscio E, Watson ME, Jr, Caparon MG. 2018. CcpA coordinates growth/damage balance for Streptococcus pyogenes pathogenesis. Sci Rep 8:14254. https://doi.org/10.1038/s41598-018-32558-0.
46. Loh JMS, Adenwalla N, Wiles S, Proft T. 2013. Galleria mellonella larvae as an infection model for group A streptococcus. Virulence 4:419–428. https://doi.org/10.4161/viru.24930.
47. Olsen RJ, Ebru Watkins M, Cantu CC, Beres SB, Musser JM. 2011. Virulence of serotype M3 group A streptococcus strains in wax worms (Galleria mellonella larvae). Virulence 2:111–119. https://doi.org/10.4161/viru.2.2.14338.
48. Evans BA, Rozen DE. 2012. A Streptococcus pneumoniae infection model in larvae of the wax moth Galleria mellonella. Eur J Clin Microbiol Infect Dis 31:2653–2660. https://doi.org/10.1007/s10096-012-1609-7.
49. Velikova N, Kavanagh K, Wells JM. 2016. Evaluation of Galleria mellonella larvae for studying the virulence of Streptococcus suis. BMC Microbiol 16:1–9. https://doi.org/10.1186/s12866-016-0905-2.
50. Cools F, Torfs E, Aizawa J, Vanhoutte B, Maes L, Caljon G, Delputte P, Cappoen D, Cos P. 2019. Optimization and characterization of a Galleria mellonella larval infection model for virulence studies and the evaluation of therapeutics against Streptococcus pneumoniae. Front Microbiol 10:311. https://doi.org/10.3389/fmicb.2019.00311.
51. Kavanagh K, Reeves EP. 2004. Exploiting the potential of insects for in vivo pathogenicity testing of microbial pathogens. FEMS Microbiol Rev 28:101–112. https://doi.org/10.1016/j.femsre.2003.09.002.
52. Wu G, Xu L, Yi Y. 2016. Galleria mellonella larvae are capable of sensing the extent of priming agent and mounting proportionatal cellular and humoral immune responses. Immunol Lett 174:45–52. https://doi.org/10.1016/j.imlet.2016.04.013.
53. Lange A, Schäfer A, Bender A, Steimle A, Beier S, Parusel R, Frick JS. 2018. Galleria mellonella: a novel invertebrate model to distinguish intestinal symbionts from pathobionts. Front Immunol 9:2114. https://doi.org/10.3389/fimmu.2018.02114.
54. Vertyporokh L, Wojda I. 2017. Expression of the insect metalloproteinase inhibitor IMPI in the fat body of Galleria mellonella exposed to infection with Beauveria bassiana. Acta Biochim Pol 64:273–278. https://doi.org/10.18388/abp.2016_1376.
55. Gandhe AS, John SH, Nagaraju J. 2007. Noduler, a novel immune up-regulated protein mediates nodulation response in insects. J Immunol 179:6943–6951. https://doi.org/10.4049/jimmunol.179.10.6943.
56. Cosson P, Soldati T. 2008. Eat, kill or die: when amoeba meets bacteria. Curr Opin Microbiol 11:271–276. https://doi.org/10.1016/j.mib.2008.05.005.
57. Jauslin T, Lamrabet O, Crespo-Yañez X, Marchetti A, Ayadi I, Ifrid E, Guilhen C, Leippe M, Cosson P. 2021. How phagocytic cells kill different bacteria: a quantitative analysis using Dictyostelium discoideum. mBio 12:e03169-20. https://doi.org/10.1128/mBio.03169-20.
58. Browne N, Heelan M, Kavanagh K. 2013. An analysis of the structural and functional similarities of insect hemocytes and mammalian phagocytes. Virulence 4:597–603. https://doi.org/10.4161/viru.25906.
59. Wei YS, Chang YR, Tsai YT, Yang YT, Weng SH, Tseng LF, Chou HC, Hu AT, Liao EC, Chen HY, Lin GY, Cheng WC, Chan HL. 2021. The distribution of cultivable oral anaerobic microbiota identified by MALDI-TOF MS in healthy subjects and in patients with periodontal disease. J Pharm Biomed Anal 192:113647. https://doi.org/10.1016/j.jpba.2020.113647.
60. Wanahita A, Goldsmith EA, Musher DM, Clarridge JE, Rubio J, Krishnan B, JoAnn Trial. 2002. Interaction between human polymorphonuclear leukocytes and Streptococcus milleri group bacteria. J Infect Dis 185:85–90. https://doi.org/10.1086/338145.
61. Pukatzki S, Kessin RH, Mekalanos JJ. 2002. The human pathogen Pseudomonas aeruginosa utilizes conserved virulence pathways to infect the social amoeba Dictyostelium discoideum. Proc Natl Acad Sci U S A 99:3159–3164. https://doi.org/10.1073/pnas.052704399.
62. Pan YJ, Lin TL, Hsu CR, Wang JT. 2011. Use of a Dictyostelium model for isolation of genetic loci associated with phagocytosis and virulence in Klebsiella pneumoniae. Infect Immun 79:997–1006. https://doi.org/10.1128/IAI.00906-10.
63. Haine ER, Moret Y, Siva-Jothy MT, Rolff J. 2008. Antimicrobial defense and persistent infection in insects. Science 322:1257–1259. https://doi.org/10.1126/science.1165265.
64. Sheehan G, Dixon A, Kavanagh K. 2019. Utilization of Galleria mellonella larvae to characterize the development of Staphylococcus aureus infection. Microbiology (Reading) 165:863–875. https://doi.org/10.1099/mic.0.000813.
65. Asai M, Sheehan G, Li Y, Robertson BD, Kavanagh K, Langford PR, Newton SM. 2021. Innate immune responses of Galleria mellonella to Mycobacterium bovis BCG challenge identified using proteomic and molecular approaches. Front Cell Infect Microbiol 11:619981. https://doi.org/10.3389/fcimb.2021.619981.

66. Iyer R, Baliga NS, Camilli A. 2005. Catabolite control protein A (CcpA) contributes to virulence and regulation of sugar metabolism in Streptococcus pneumoniae. J Bacteriol 187:8340–8349. https://doi.org/10.1128/JB.187.24.8340-8349.2005.
67. Shelburne SA, Keith D, Horstmann N, Sumby P, Davenport MT, Graviss EA, Brennan RG, Musser JM. 2008. A direct link between carbohydrate utilization and virulence in the major human pathogen group A streptococcus. Proc Natl Acad Sci U S A 105:1698–1703. https://doi.org/10.1073/pnas.0711767105.
68. Zheng L, Chen Z, Itzek A, Herzberg MC, Kreth J. 2012. CcpA regulates biofilm formation and competence in Streptococcus gordonii. Mol Oral Microbiol 27:83–94. https://doi.org/10.1111/j.2041-1014.2011.00633.x.
69. Kinkel TL, McIver KS. 2008. CcpA-mediated repression of streptolysin S expression and virulence in the group A streptococcus. Infect Immun 76:3451–3463. https://doi.org/10.1128/IAI.00343-08.
70. Shelburne SA, Davenport MT, Keith DB, Musser JM. 2008. The role of complex carbohydrate catabolism in the pathogenesis of invasive streptococci. Trends Microbiol 16:318–325. https://doi.org/10.1016/j.tim.2008.04.002.
71. Six A, Krajangwong S, Crumlish M, Zadoks RN, Walker D. 2019. Galleria mellonella as an infection model for the multi-host pathogen Streptococcus agalactiae reflects hypervirulence of strains associated with human invasive disease. Virulence 10:600–609. https://doi.org/10.1080/21505594.2019.1631660.
72. Del Pilar Crespo-Ortiz M, Burbano ME, Barreto M. 2020. Pathogenesis and in vivo interactions of human Streptococcus agalactiae isolates in the Galleria mellonella invertebrate model. Microb Pathog 147:104400. https://doi.org/10.1016/j.micpath.2020.104400.
73. Dangel ML, Dettmann JC, Haßelbarth S, Krogull M, Schakat M, Kreikemeyer B, Fiedler T. 2019. The 5′-nucleotidase S5nA is dispensable for evasion of phagocytosis and biofilm formation in Streptococcus pyogenes. PLoS One 14:e0211074. https://doi.org/10.1371/journal.pone.0211074.
74. Tsai CJ-Y, Loh JMS, Proft T. 2020. The use of Galleria mellonella (wax moth) as an infection model for group A streptococcus. Methods Mol Biol 2136:279–286. https://doi.org/10.1007/978-1-0716-0467-0_21.
75. Avilés-Reyes A, Miller JH, Simpson-Haidaris PJ, Lemos JA, Abranches J. 2014. Cnm is a major virulence factor of invasive Streptococcus mutans and part of a conserved three-gene locus. Mol Oral Microbiol 29:11–23. https://doi.org/10.1111/omi.12041.
76. Buckley AA, Faustoferri RC, Quivey RG. 2014. β-Phosphoglucomutase contributes to aciduricity in Streptococcus mutans. Microbiology (Reading) 160:818–827. https://doi.org/10.1099/mic.0.075754-0.
77. Smoot LM, Smoot JC, Graham MR, Somerville GA, Sturdevant DE, Migliaccio CA, Sylva GL, Musser JM. 2001. Global differential gene expression in response to growth temperature alteration in group A streptococcus. Proc Natl Acad Sci U S A 98:10416–10421. https://doi.org/10.1073/pnas.191267598.
78. Mereghetti L, Sitkiewicz I, Green NM, Musser JM. 2008. Remodeling of the Streptococcus agalactiae transcriptome in response to growth temperature. PLoS One 3:e2785. https://doi.org/10.1371/journal.pone.0002785.
79. Pandya U, Allen CA, Watson DA, Niesel DW. 2005. Global profiling of Streptococcus pneumoniae gene expression at different growth temperatures. Gene 360:45–54. https://doi.org/10.1016/j.gene.2005.06.023.
80. Nathan S. 2014. New to Galleria mellonella: modeling an ExPEC infection. Virulence 5:371–374. https://doi.org/10.4161/viru.28338.
81. Kwadha CA, Ong'Amo GO, Ndegwa PN, Raina SK, Fombong AT. 2017. The biology and control of the greater wax moth, Galleria mellonella. Insects 8:61. https://doi.org/10.3390/insects8020061.
82. Desalermos A, Fuchs BB, Mylonakis E. 2012. Selecting an invertebrate model host for the study of fungal pathogenesis. PLoS Pathog 8:e1002451. https://doi.org/10.1371/journal.ppat.1002451.
83. Obszańska K, Kern-Zdanowicz I, Kozińska A, Machura K, Stefaniuk E, Hryniewicz W, Sitkiewicz I. 2016. Streptococcus anginosus (milleri) group strains isolated in Poland (1996–2012) and their antibiotic resistance patterns. Pol J Microbiol 65:33–41. https://doi.org/10.5604/17331331.1197323.
84. Obszańska K, Kern-Zdanowicz I, Sitkiewicz I. 2018. Efficient construction of Streptococcus anginosus mutants in strains of clinical origin. J Appl Genet 59:515–523. https://doi.org/10.1007/s13353-018-0468-z.
85. Lukomski S, Hoe NP, Abdi I, Rurangirwa J, Kordari P, Liu M, Dou SJ, Adams GG, Musser JM. 2000. Nonpolar inactivation of the hypervariable streptococcal inhibitor of complement gene (sic) in serotype M1 Streptococcus pyogenes significantly decreases mouse mucosal colonization. Infect Immun 68:535–542. https://doi.org/10.1128/IAI.68.2.535-542.2000.
86. Shariff A, Luna EJ. 1990. Dictyostelium discoideum plasma membranes contain an actin-nucleating activity that requires ponticulin, an integral membrane glycoprotein. J Cell Biol 110:681–692. https://doi.org/10.1083/jcb.110.3.681.
87. Wojda I, Jakubowicz T. 2007. Humoral immune response upon mild heat-shock conditions in Galleria mellonella larvae. J Insect Physiol 53:1134–1144. https://doi.org/10.1016/j.jinsphys.2007.06.003.
88. Dubovskiy IM, Grizanova EV, Whitten MMA, Mukherjee K, Greig C, Alikina T, Kabilov M, Vilcinskas A, Glupov VV, Butt TM. 2016. Immuno-physiological adaptations confer wax moth Galleria mellonella resistance to Bacillus thuringiensis. Virulence 7:860–870. https://doi.org/10.1080/21505594.2016.1164367.
89. Livak KJ, Schmittgen TD. 2001. Analysis of relative gene expression data using real-time quantitative PCR and the 2(-Delta Delta C(T)) method. Methods 25:402–408. https://doi.org/10.1006/meth.2001.1262.